Supplement to: "The added value of Med-CORDEX Coupled High-Resolution Regional Climate Models in representing Sea Surface Temperature and Marine Heatwaves in the Mediterranean Sea"

Francesco De Rovere[1], Giulia Bonino[1], Ronan McAdam[1], Enrico Scoccimarro[1], Samuel Somot[2], Iván M. Parras-Berrocal[2], Bodo Ahrens[3], Vladimir Djurdjevic[4], Laurent Li[5], and Simona Masina[1]

[1]CMCC Foundation - Euro-Mediterranean Center on Climate Change, Italy
[2]Météo-France, CNRS, Univ. Toulouse, CNRM, France
[3]Institute for Atmospheric and Environmental Sciences, Goethe University Frankfurt, Germany
[4]Faculty of Physics, University of Belgrade, Serbia
[5]Laboratoire de Météorologie Dynamique, CNRS, Sorbonne Université, Paris

Correspondence: Francesco De Rovere (francesco.derovere@cmcc.it)

Abstract. Marine heatwaves (MHWs) pose significant threats to Mediterranean marine ecosystems and coastal economies, and their frequency and severity are projected to increase under future climate change. In this context, coupled climate simulations are valuable tools to accurately characterize the properties of future MHWs in the Mediterranean. While Med-CORDEX fully-coupled Regional Climate System Models (RCSMs) offer enhanced resolution and improved representation of local processes relative to their parent Global Climate Models (GCMs), a systematic assessment of their added value for sea surface temperature (SST) and MHW properties has been lacking. This study quantifies the added value of Med-CORDEX RCSMs over the Mediterranean basin, evaluating their capacity to correct GCM biases and improve the spatiotemporal representation of SST and MHW probability distributions. Results show that added value is scale-dependent and metric-specific. RCSMs generally improve the SST spatial pattern and the shape and upper tail of its temporal distribution, but mostly fail to correct Mediterranean basin-averaged errors in the mean, standard deviation, 90th percentile and linear trend. For MHW duration, downscaling provides consistent and spatially widespread improvements across nearly all models, driven by a better representation of short-lived events. For MHW intensity, added value is model-dependent and not systematic: while the majority of RCSMs improve this metric, some models exhibit deterioration linked to model-specific features. These results demonstrate that higher horizontal resolution is a necessary but not sufficient condition for improved MHW representation, and that simultaneous advances in other model components are required to fully exploit the potential of regional downscaling.

This document includes Table S1 and Figures from S1 to S16.

Table S1. Observational and reanalysis products used in this study.

Product name	Abbreviation	Type	Hor. Res.	Frequency	Period	Description	Reference
Mediterranean Sea High Resolution and Ultra High Resolution SST Analysis	L4-SST	L4 satellite	1/16°	Daily	1982–present	Night-time foundation SST	Pisano et al. (2016); Embury et al. (2024)
Mediterranean Sea High Resolution Diurnal Subskin SST Analysis	SubSkinT	L4 satellite	1/16°	Hourly	2019–present	Sub-skin SST including diurnal cycle	Marullo et al. (2014); Buongiorno Nardelli et al. (2013)
Mediterranean Sea Physics Reanalysis	MEDREA	Ocean reanalysis	1/24°	Daily	1987–2022	Reanalysed SST and ocean state	Escudier et al. (2021)

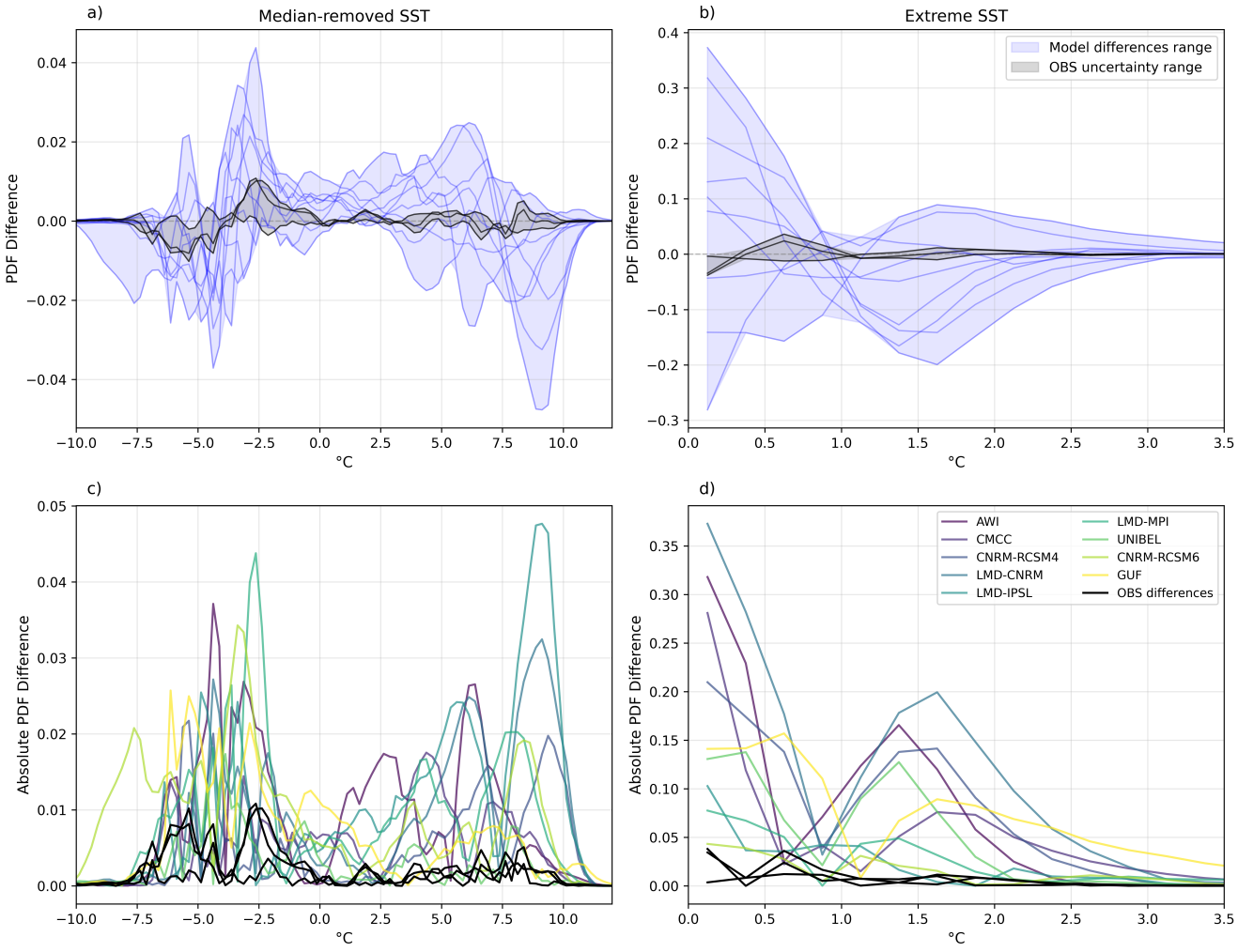

Figure S1. Comparison of PDF differences between RCSM–GCM pairs and among observational products, for median-removed SST (left column) and extreme SST (right column). Top row: PDF differences; bottom row: absolute PDF differences. The data period is from 2019 to 2022.

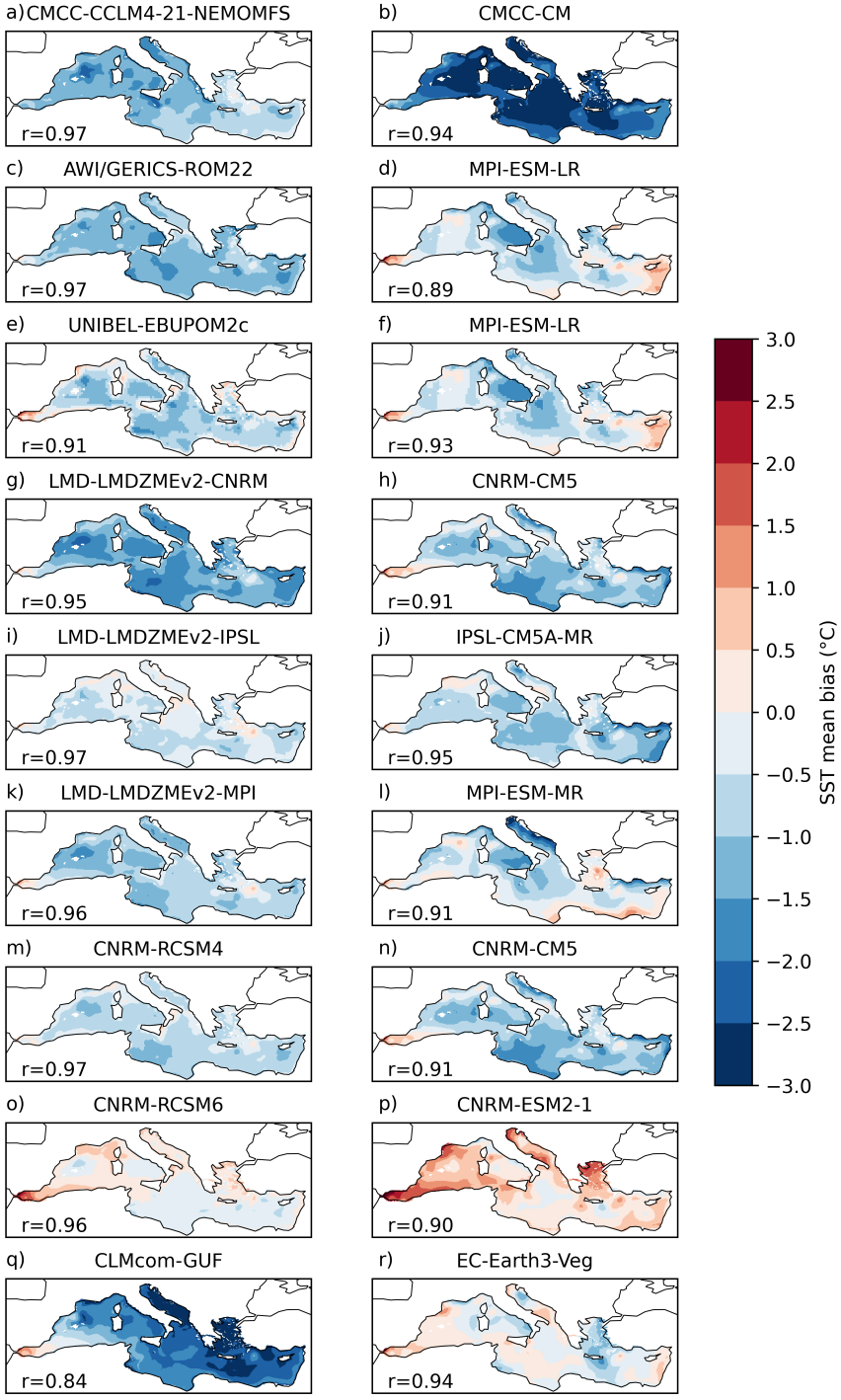

Figure S2. Mean SST biases for the RCSM (left column) and GCM (right column). The pattern correlation of mean SST maps between each model and OBS is shown in each panel.

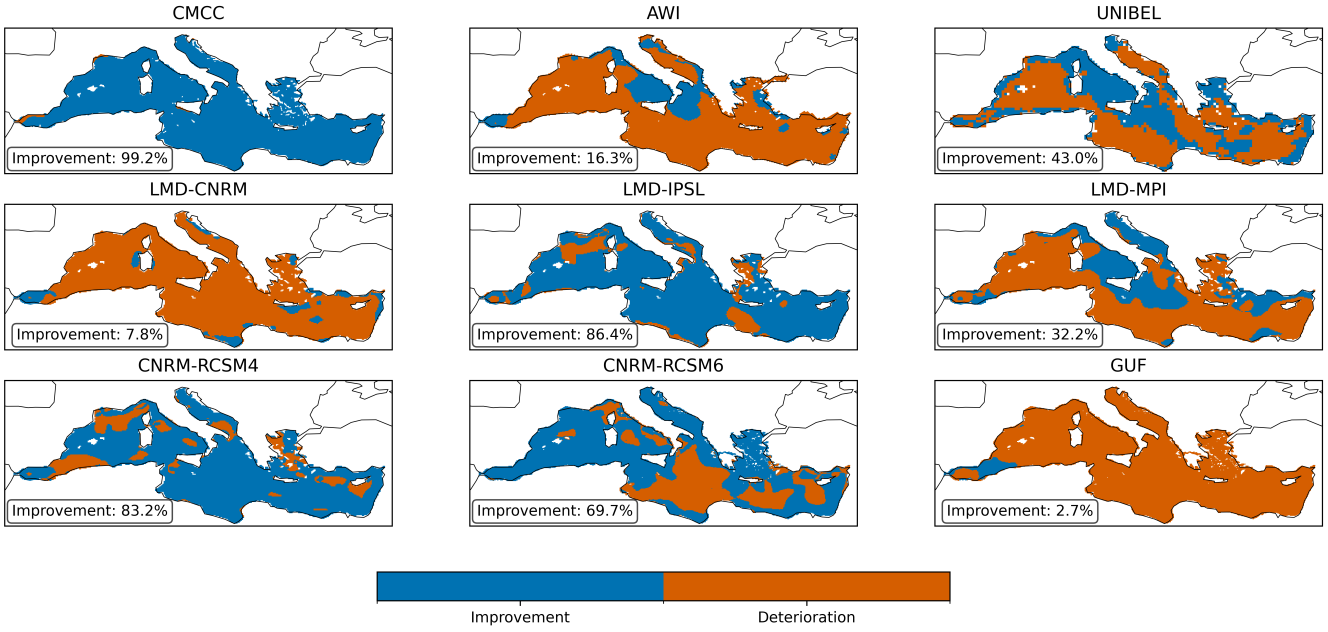

Figure S3. Spatial distribution of mean SST bias improvement for each RCSM. Blue (orange) grid points indicate where the RCSM absolute bias is lower (higher) than that of the driving GCM. The fraction of improved grid points is reported in each panel.

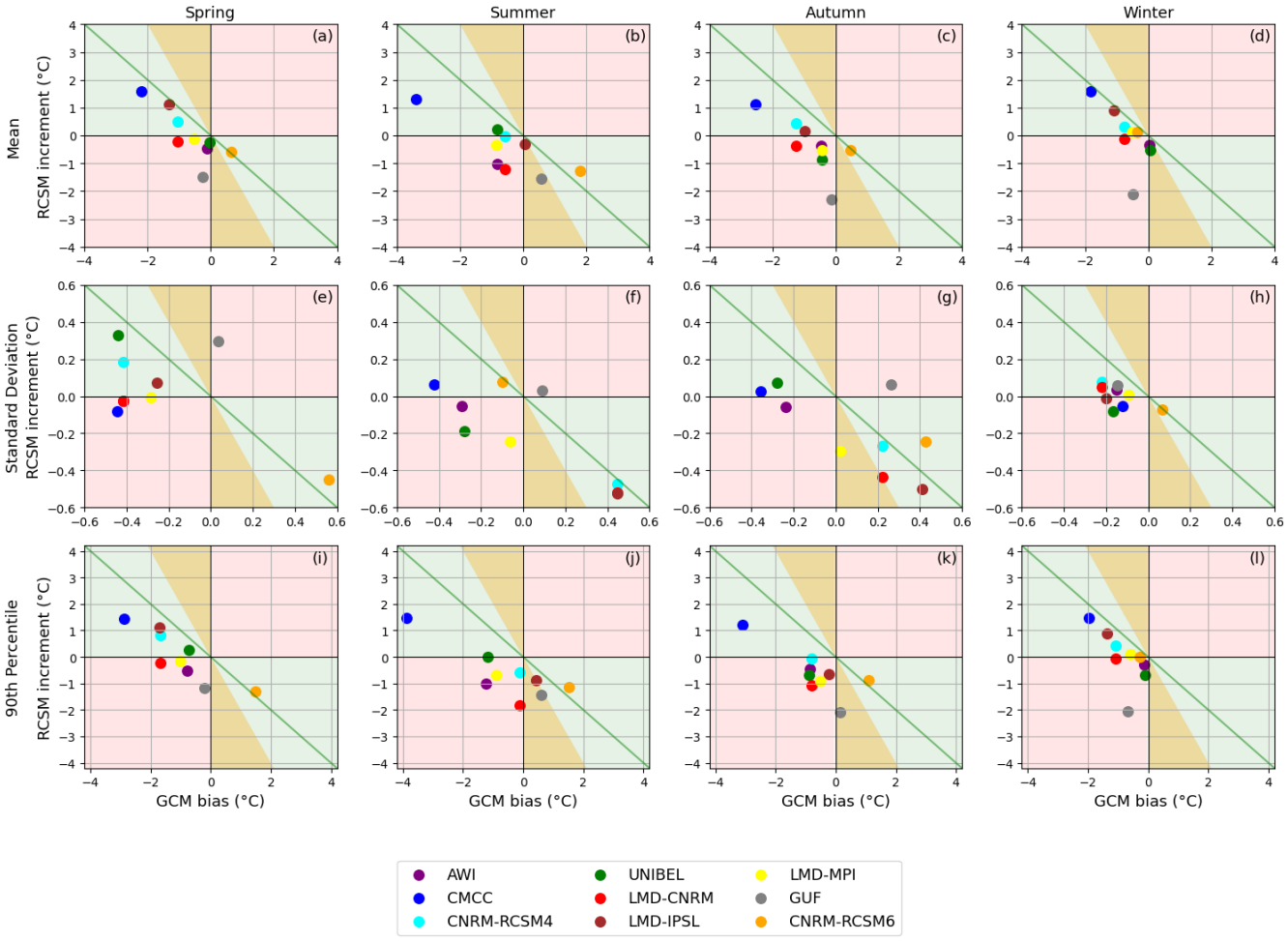

Figure S4. RCSMs increment vs GCM bias, formatted as in Figure 1 of the manuscript for area-averaged SST (a,b,c,d) mean, (e,f,g,h) standard deviation and (i,j,k,l), for (a,e,i) spring, (b,f,j) summer, (c,g,k) autumn and (d,h,l) winter in 1982-2020.

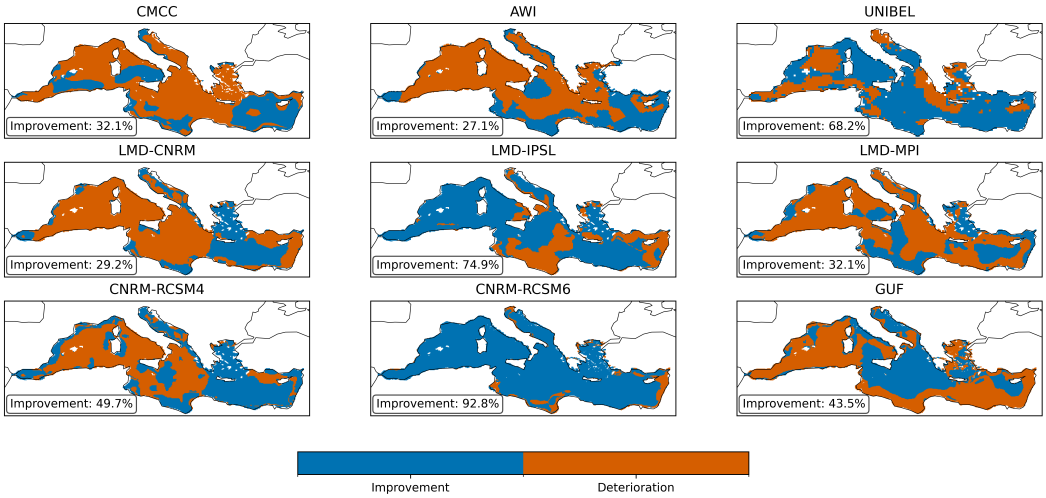

Figure S5. As in Figure S3, but for the standard deviation of SST.

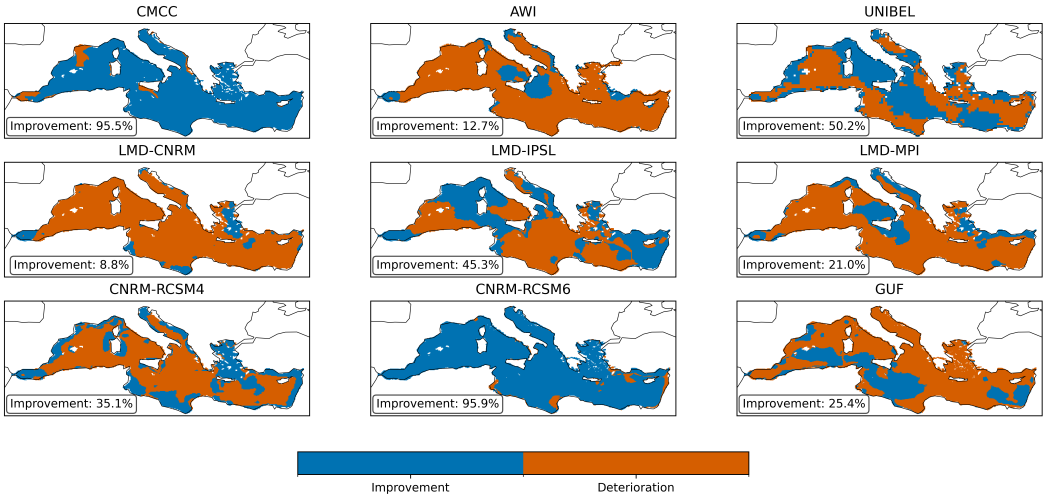

Figure S6. As in Figure S3, but for the SST 90th percentile.

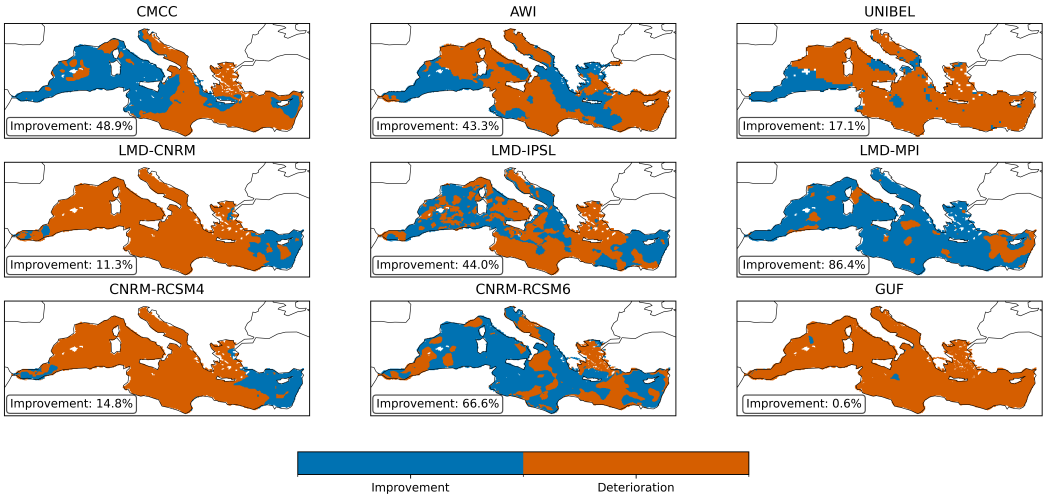

Figure S7. As in Figure S3, but for the SST trend.

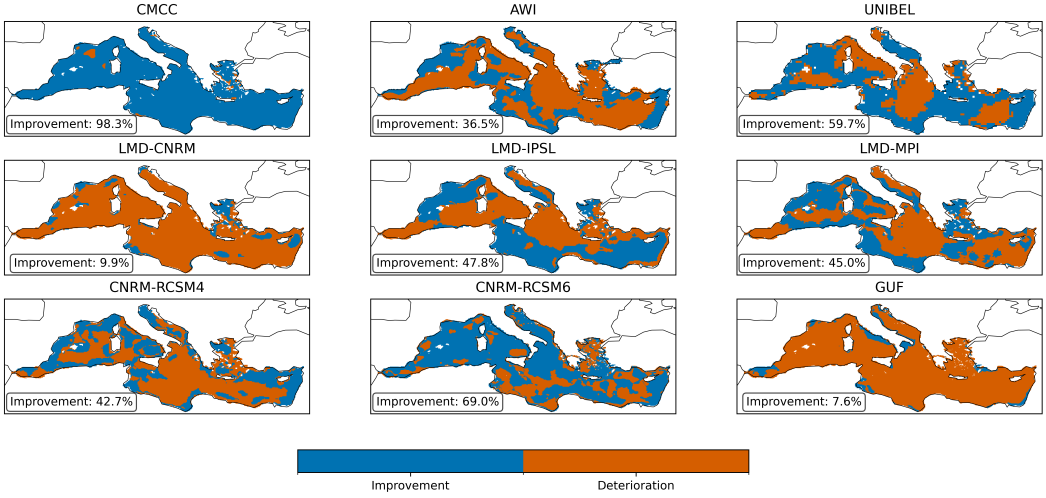

Figure S8. As in Figure S3, but for the standard deviation of SST residuals.

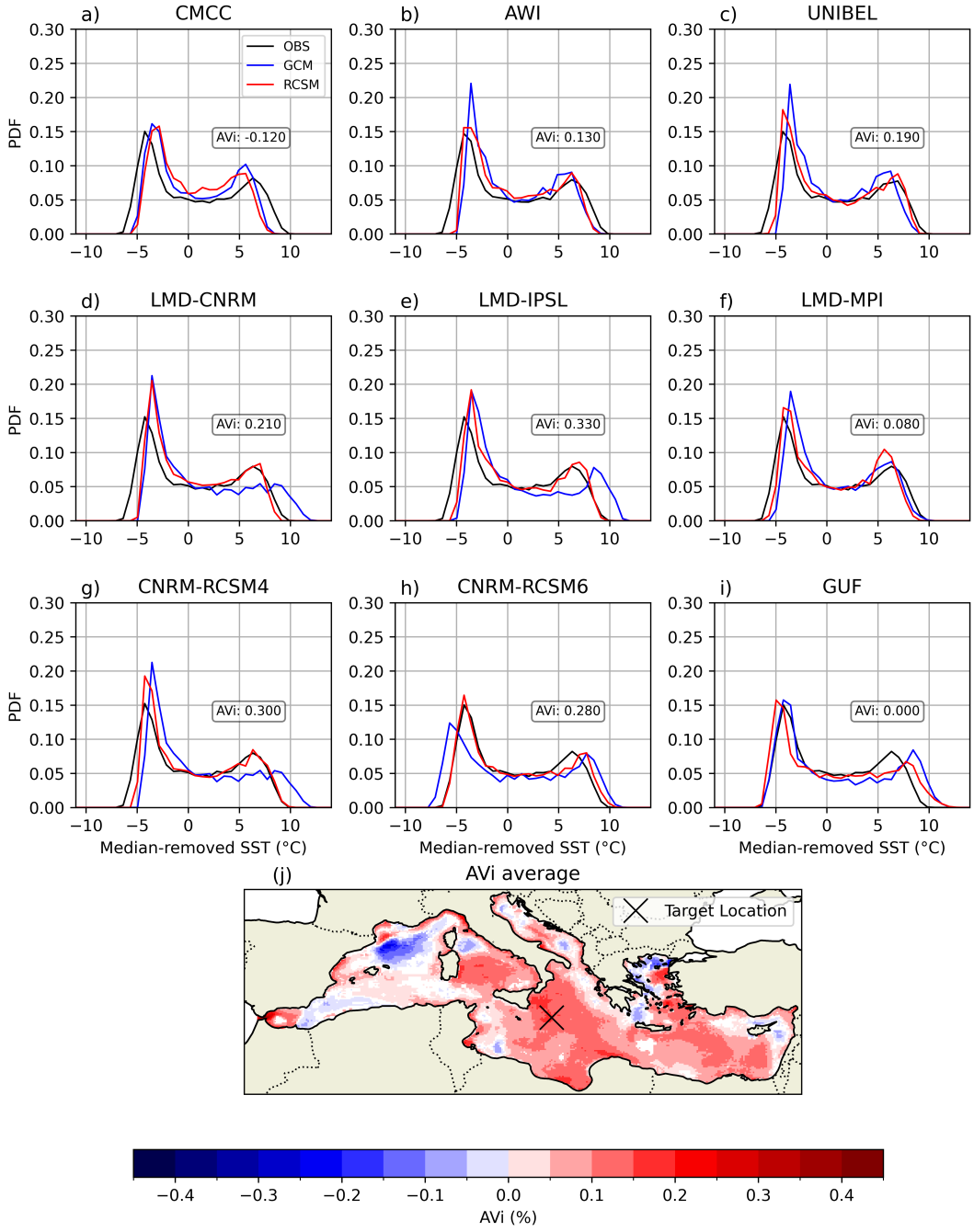

Figure S9. PDFs of median-removed SST at a point in the central Mediterranean (36° N, 17° E) for (a) CMCC, (b) AWI, (c) UNIBEL, (d) LMD-CNRM, (e) LMD-IPSL, (f) LMD-MPI, (g) CNRM-RCSM4, (h) CNRM-RCSM6, and (i) GUF. Lines show observations (black), RCSMs (red), and driving GCMs (blue). Panel j) shows the multi-model AVi mean (as in Figure 2 of the manuscript.

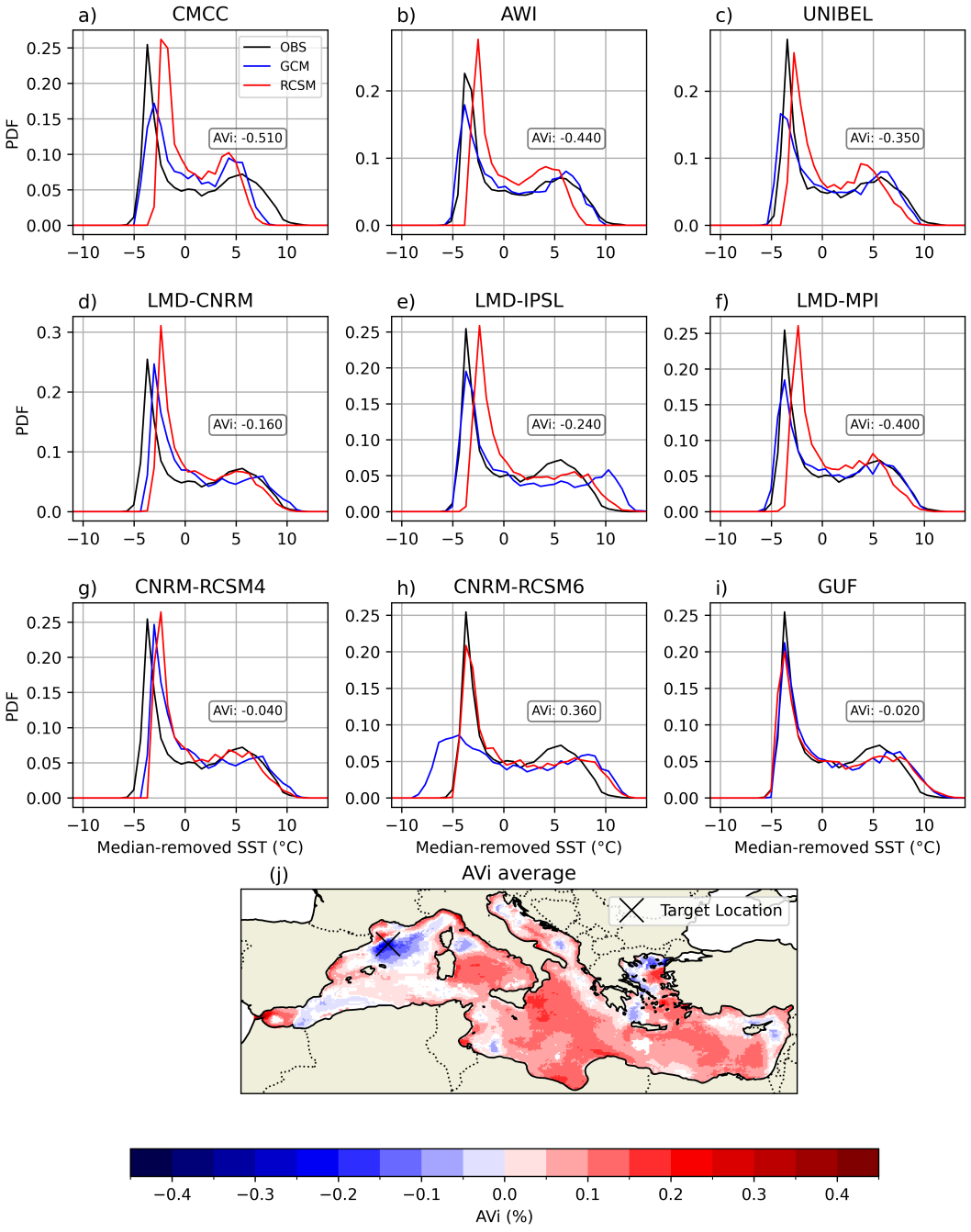

Figure S10. As in Figure S9 but for a point in the Gulf of Lion (41.7° N, 4.5° E).

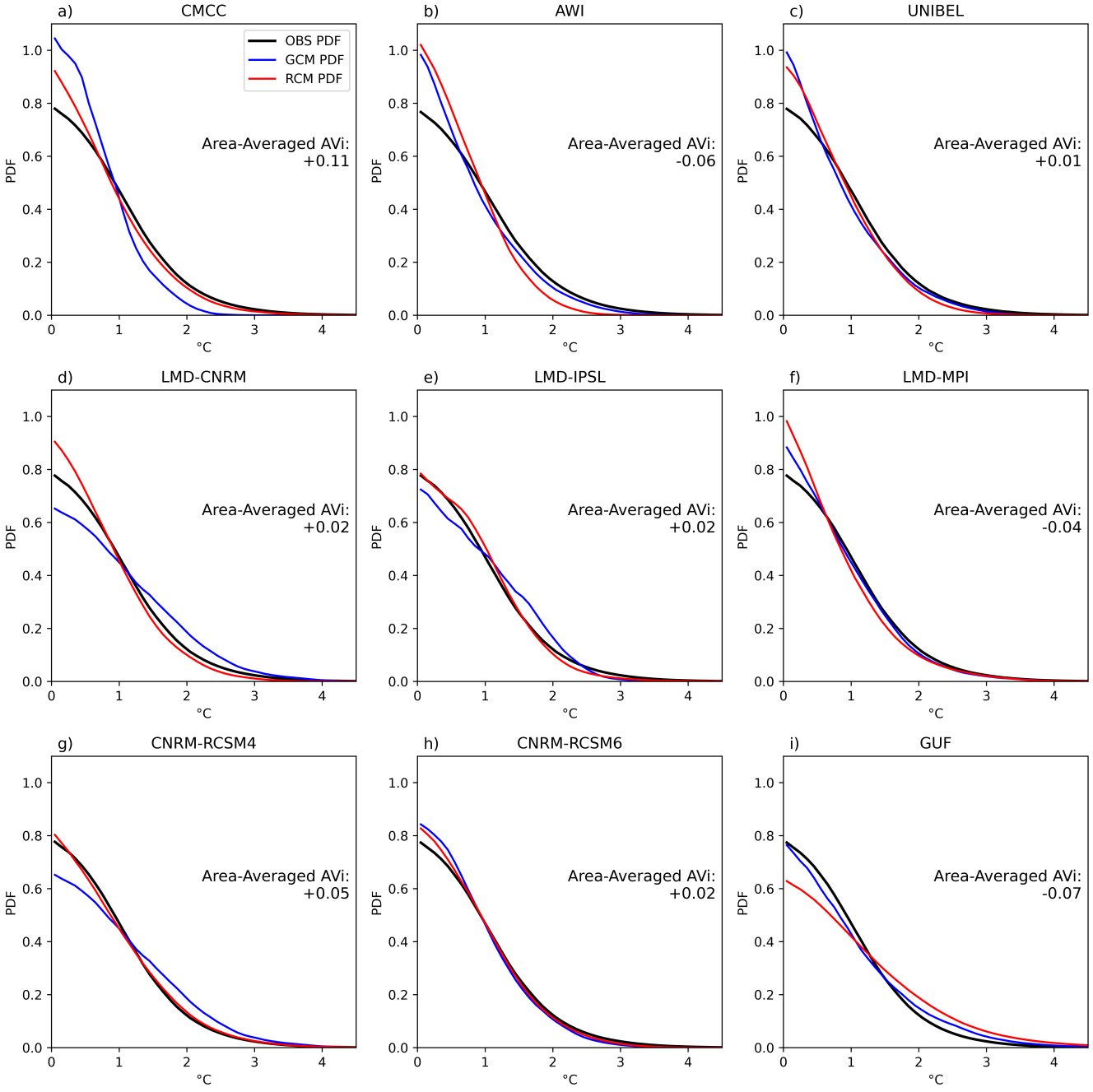

Figure S11. PDFs of upper tail SST (anomalies above the 90th percentile) for (a) CMCC, (b) AWI, (c) UNIBEL, (d) LMD-CNRM, (e) LMD-IPSL, (f) LMD-MPI, (g) CNRM-RCSM4, (h) CNRM-RCSM6, and (i) GUF. Lines show observations (black), RCSMs (red), and driving GCMs (blue). PDFs are computed by aggregating data from all grid points in the Mediterranean basin.

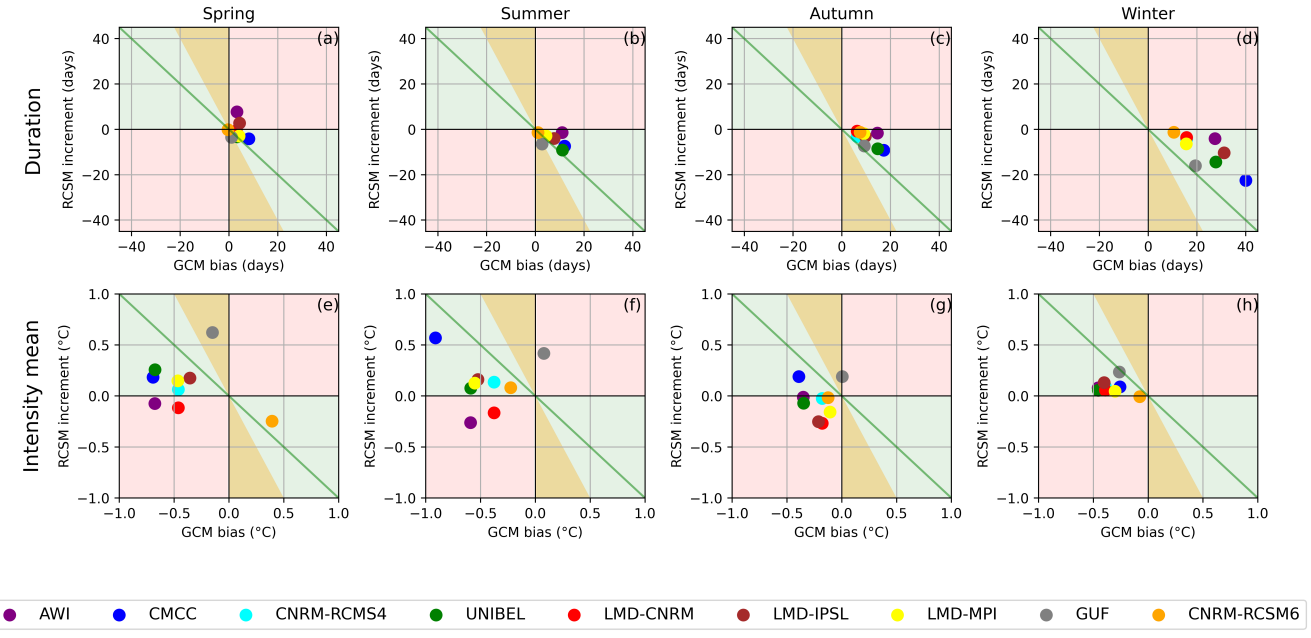

Figure S12. As in Figure S4 but for area-averaged MHW properties, calculated using a fixed baseline in 1982-2011.

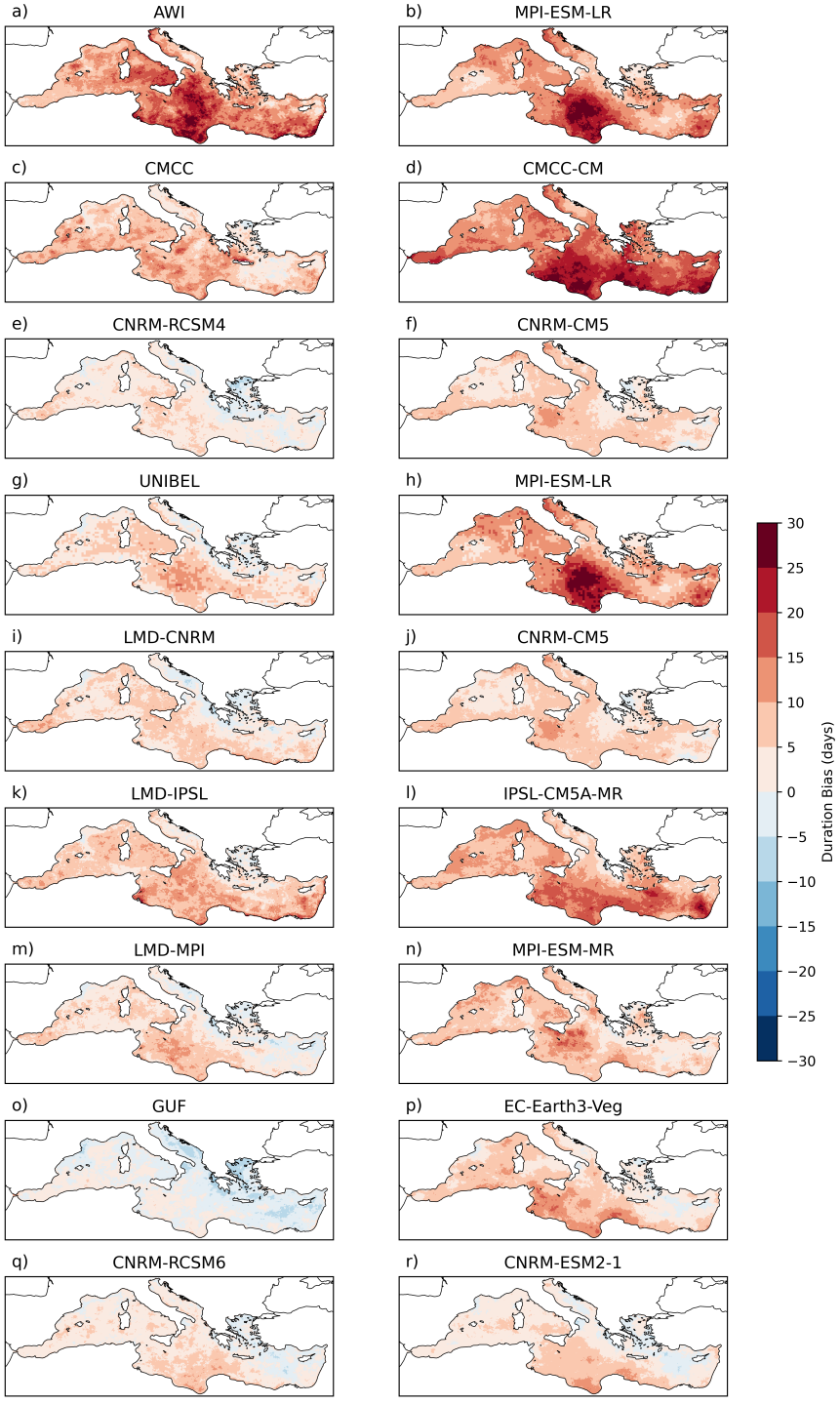

Figure S13. Mean biases in MHW duration for the RCSM (left column) and GCM (right column). MHWs are calculated using a fixed baseline in 1982-2011.

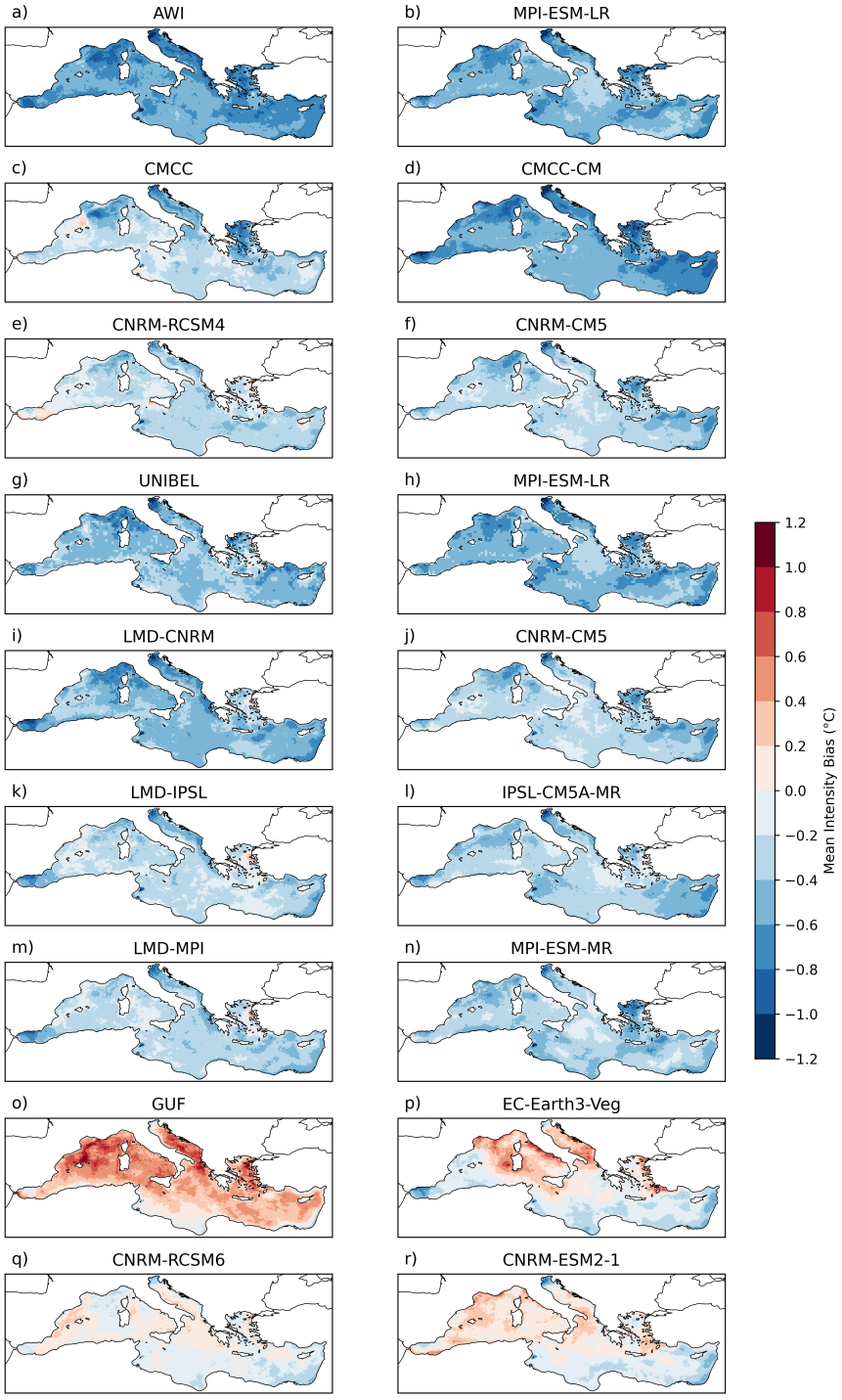

Figure S14. As in Figure SS13 but for MHW intensity.

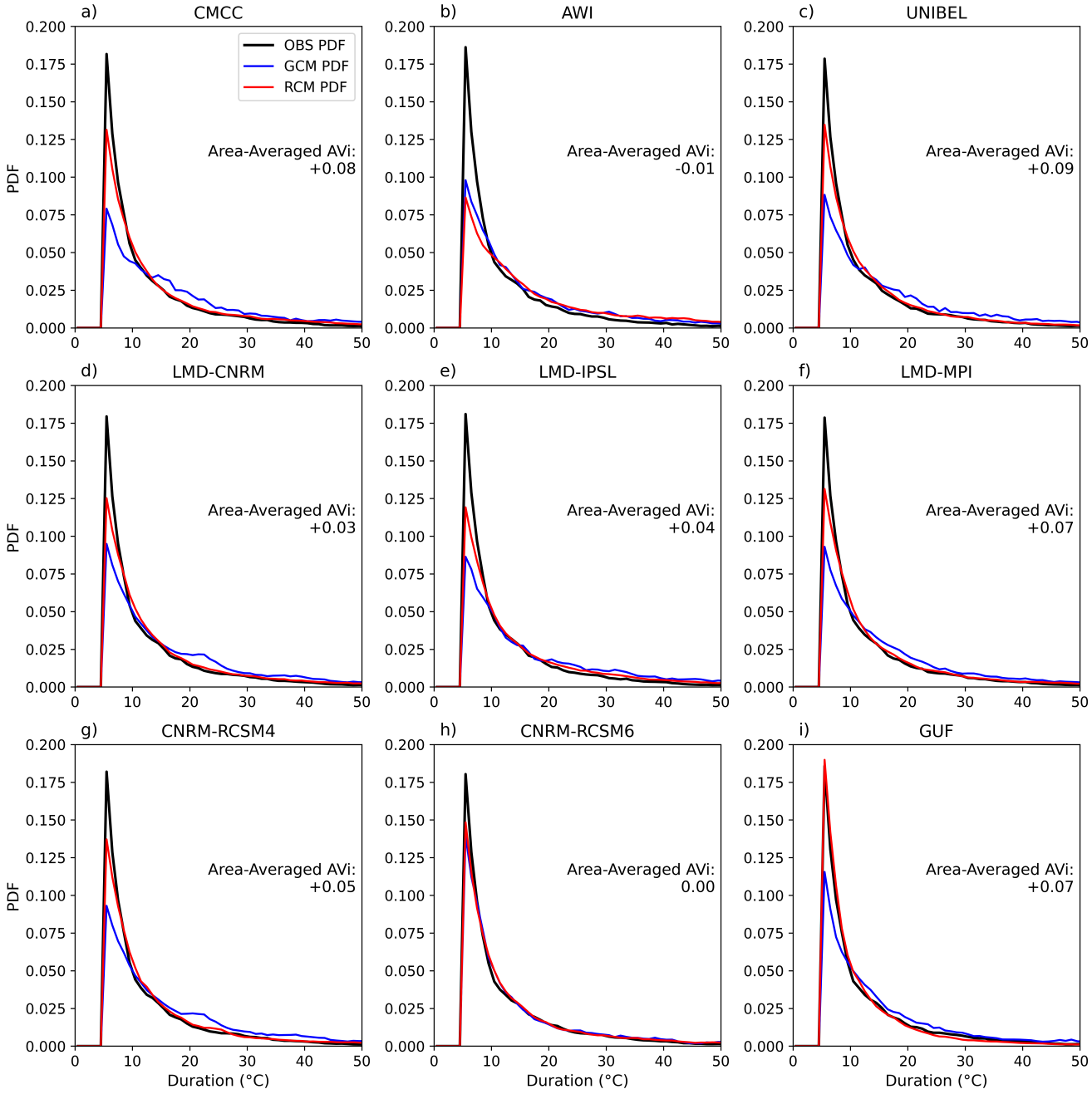

Figure S15. PDFs of aggregated MHW durations over AVi significant grid points for (a) CMCC, (b) AWI, (c) UNIBEL, (d) LMD-CNRM, (e) LMD-IPSL, (f) LMD-MPI, (g) CNRM-RCSM4, (h) CNRM-RCSM6, and (i) GUF. Lines show observations (black), RCSMs (red), and driving GCMs (blue).

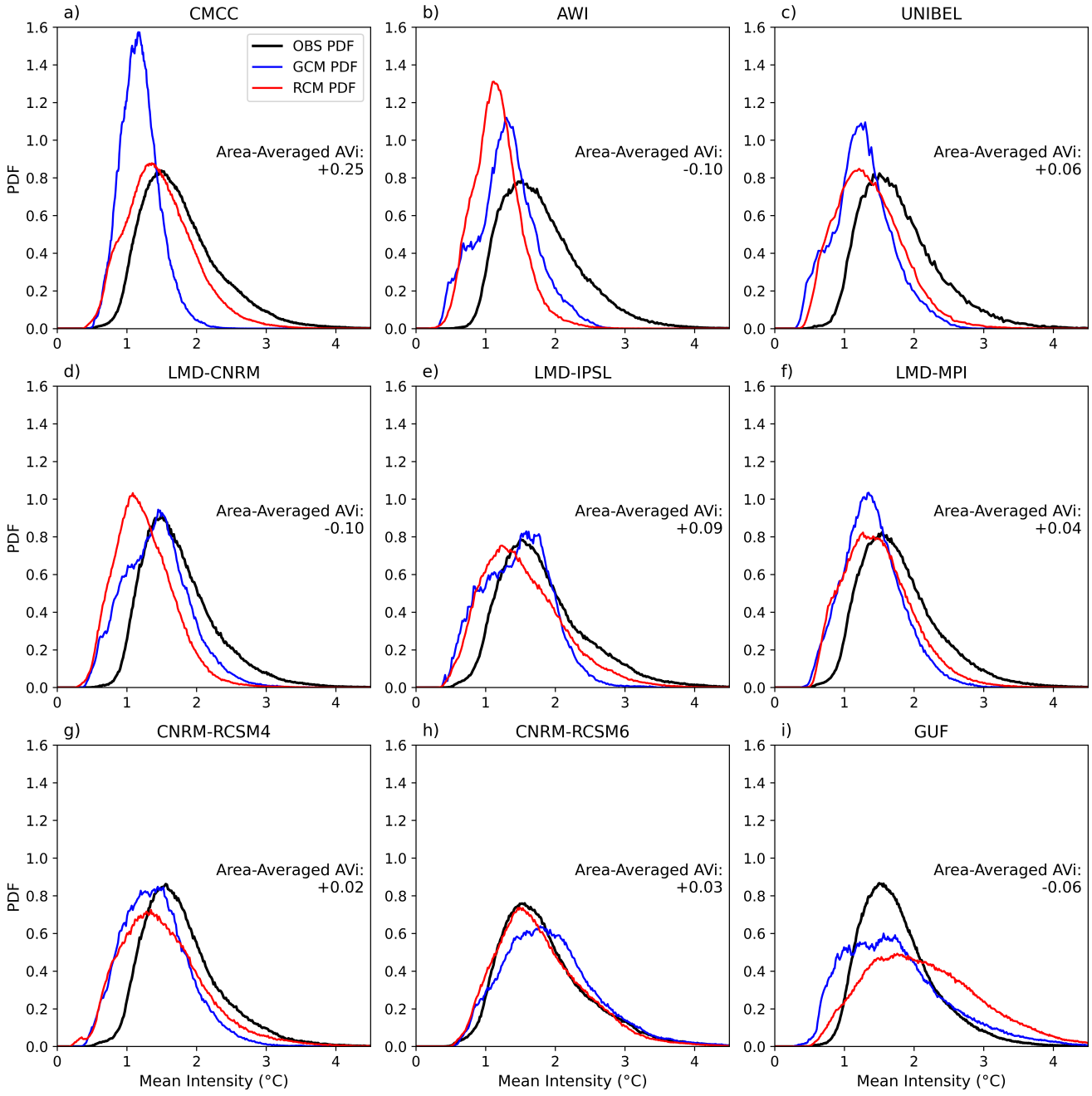

Figure S16. As in Figure SS15 but for MHW mean intensity.

References

References

Buongiorno Nardelli, B., Tronconi, C., Pisano, A., and Santoleri, R.: High and Ultra-High resolution processing of satellite Sea Surface Temperature data over Southern European Seas in the framework of MyOcean project, 129, 1–16, https://doi.org/10.1016/j.rse.2012.10.012, 2013.

Embury, O., Merchant, C. J., Good, S. A., Rayner, N. A., Høyer, J. L., Atkinson, C., Block, T., Alerskans, E., Pearson, K. J., Worsfold, M., McCarroll, N., and Donlon, C.: Satellite-based time-series of sea-surface temperature since 1980 for climate applications, Scientific Data, 11, 326, https://doi.org/10.1038/s41597-024-03147-w, 2024.

Escudier, R., Clementi, E., Cipollone, A., Pistoia, J., Drudi, M., Grandi, A., Lyubartsev, V., Lecci, R., Aydogdu, A., Delrosso, D., Omar, M., Masina, S., Coppini, G., and Pinardi, N.: A High Resolution Reanalysis for the Mediterranean Sea, 9, 702 285, https://doi.org/10.3389/feart.2021.702285, 2021.

Marullo, S., Santoleri, R., Ciani, D., Le Borgne, P., Péré, S., Pinardi, N., Tonani, M., and Nardone, G.: Combining model and geostationary satellite data to reconstruct hourly SST field over the Mediterranean Sea, 146, 11–23, https://doi.org/10.1016/j.rse.2013.11.001, 2014.

Pisano, A., Buongiorno Nardelli, B., Tronconi, C., and Santoleri, R.: The new Mediterranean optimally interpolated pathfinder AVHRR SST Dataset (1982–2012), Remote Sensing of Environment, 176, 107–116, https://doi.org/10.1016/j.rse.2016.01.019, 2016.